Journal of Magnetic Resonance 209 (2011) 109–115

Contents lists available at ScienceDirect

Journal of Magnetic Resonance

journal homepage: www.elsevier.com/locate/jmr

Perspectives in Magnetic Resonance

Advances in bio-imaging: A survey from WWMR 2010

Silvio Aime *, Francesca Reineri

Dept. of Chemistry I.F.M. and Centre of Molecular Imaging, University of Torino, via P. Giuria 7 10125 Torino, Italy

ARTICLE INFO

Article history:
Received 24 January 2011
Revised 9 February 2011
Available online 3 March 2011

Keywords:
MRI
Hyperpolarization
Molecular Imaging
MRI Acquisition Methods

ABSTRACT

The paper deals with a survey on major advances in the field of bio-imaging presented at the WWMR2010 Conference, held in Florence (Italy) from 4th to 9th July 2010. The selected contributions have been organized into the following headings: Hyperpolarization, Acquisition Methods and Molecular Imaging applications. Overall, the Conference has witnessed an outstanding progress in either methods and applications that further stresses the key-role of MRI in many fields of biomedicine.

0. Introduction

The World Wide Magnetic Resonance (WWMR) 2010 Conference (held in Florence, July 4–9, 2010) gathered ca. 1500 participants and covered all the major topics in the NMR, MRI and ESR fields. We have been asked by the organizers to survey the most relevant advances in fields related to bio-imaging that were presented at the conference. Obviously such selection is not easy because of the very high quality of most of the oral and poster contributions and the subjective limits and interests of the reviewers. With the selected contributions, we hope to offer the reader an overall view of the Florence meeting that witnesses how NMR is a key tool for the development of understanding in biology and medicine. The survey is been organized under three main headings: hyperpolarization, acquisition methods, and molecular imaging applications. We apologize in advance for any undue omission.

1. Hyperpolarization

As noted by Robert Griffin in his ISMAR Price Lecture, there has been a renaissance in hyperpolarization due to advances including new instrumentation, new hyperpolarized agents tailored for specific experiments, and magnetic resonance methodology. Advances in hyperpolarization have been some of the most important achievements in the field of biomedical applications reported in this survey.

All the main hyperpolarization techniques—optically pumped noble gases, DNP (dynamic nuclear polarization) hyperpolarized molecules, and parahydrogen-induced polarization were tackled and their potential applications for improved bio-imaging stressed at the conference.

1.1. Hyperpolarized noble gases

The application of hyperpolarized noble gases (^{3}He and ^{129}Xe) was first introduced to obtain MR images of airspace anatomy for indirect visualization of pathological conditions [1,2]. The newest development in this field allows the characterization of lung microstructure at the alveolar level by measurement of the apparent diffusion coefficient (ADC) using hyperpolarized ^{3}He [3]. ADC images, which make it possible to detect tissue destruction from chronic obstructive pulmonary disease (COPD), rely on the fact that diffusion of gases into alveoli is strongly limited relative to free diffusion. As this disease generates increased alveolar size, significant differences in ADC values have been measured between healthy subjects and subjects affected by emphysema. Pathological lung structures are also described by alveolar partial pressure of oxygen (pO_2) and oxygen depletion rate (R). The use of hyperpolarized ^{3}He provides a way to measure pO_2 and R, as the relaxation rate of the polarized nucleus is increased by the presence of paramagnetic oxygen, yielding a kind of functional lung imaging using hyperpolarized gas. The correlation between pulmonary structure and oxygen exchange efficiency is particularly interesting for the early diagnosis of disease and for detection of response to treatment. Recently Rizi and co-workers [4] have introduced a measurement technique that makes it possible to obtain ADC, pO_2, and R from the same measurement. This makes it possible to save expensive ^{3}He, to apply shorter measurement times, and to assess the correlation between all the parameters related to COPD.

Hyperpolarized ^{3}He has been preferred to ^{129}Xe for its greater magnetic moment and its lower relaxation rate. However, because of the limited availability of ^{3}He and its very high cost, development of hyperpolarized ^{129}Xe utilization in MRI is still very desirable. Progress in ^{129}Xe imaging was reported using a continuous flow polarizer that can deliver a dilute mixture of polarized ^{129}Xe

* Corresponding author. Fax: +39 011 6707855.
E-mail address: silvio.aime@unito.it (S. Aime).

1090-7807/$ - see front matter © 2011 Elsevier Inc. All rights reserved.
doi:10.1016/j.jmr.2011.02.021

[5,6]. The possibility of supplying multiple doses of polarized Xe enables imaging of the airspace with good resolution. More interestingly, the solubility of Xe in blood and lipid-rich tissues allows perfusion imaging in brain, lung, and other tissues. Spectroscopy studies take advantage of the large chemical shift difference between Xe in the airspace and Xe dissolved in lung tissue and in blood. Several diseases that alter the thickness of lung tissues can be investigated by means of Xe diffusion.

Innovative ideas have been also introduced for pursuing early diagnosis of lung micrometastases based on the use of hyperpolarized gases in the presence of paramagnetic nanoparticles (SPION) [7]. These particles generate strong local gradients of magnetic susceptibility that, in turn, induce very fast polarization decay. Thanks to functionalization with biologically active ligands capable of recognizing specific target molecules, these paramagnetic particles can be accumulated at lung metastases at an early stage of the disease, and their presence can then be detected by assessing the polarization decay of hyperpolarized ^{3}He or ^{129}Xe.

The application of hyperpolarized Xe is not limited to acquisition of anatomical images of void spaces such as those in the lungs. The Larmor frequency of this noble gas displays high sensitivity to the molecular environment, a property that has already been extensively exploited in the study of microporous materials. Pines and co-workers [8] suggested a method that takes advantage of this property and allows the application of hyperpolarized Xe as a biosensor. For this application, Xe is encapsulated in molecular cages that are suitably functionalized to recognize specific molecular targets. The biosensing capability of functionalized Xe-containing cages can then be combined with the spatial encoding provided by MRI. The direct application of this type of biosensor to molecular imaging is not possible, because in vivo only a small fraction of Xe is associated with the cage and the corresponding Xe signal is considerably broadened in heterogeneous samples. To overcome this drawback, an interesting development of this approach was introduced [9]. It takes advantage of chemical exchange between the pool of free Xe and the Xe encapsulated in the biosensor cage. This technique is analogous to chemical exchange saturation transfer applied to proton imaging, and it has therefore been called HYPER-CEST (CEST = chemical exchange saturation transfer). In the proposed experimental setup the intensity of the larger free Xe pool is detected by applying a saturation RF field at the absorption frequency of the targeted Xe biosensor. HYPER-CEST is a highly sensitive method that reports on active sites. As the detected hyperpolarized nucleus is not covalently bound to the biosensor, the functionalized cryptophane cage can be delivered into tissues and accumulated well before the injection of hyperpolarized Xe.

At WWMR2010 it was also reported that hyper-CEST can be exploited in NMR thermometry [10,11]. This application relies on the fact that temperature variations modify the strength of the interaction within the cage and the exchange rate between free and encapsulated Xe. Linear dependence of the chemical shift of the encapsulated Xe on temperature has been shown. It is possible to discriminate, in a phantom, regions having a 0.1 °C temperature difference using a sensor concentration of 150 μM.

Another development of the Hyper-CEST methodology dealt with the use of functionalized viral capsids as carriers for Xe sensors [12]. The coat protein of a virus has a porous structure that can incorporate several Xe-containing cages. Viral capsids can be targeted to specific epitopes, thus allowing selective detection of very low concentration of molecular targets. The targeting sensitivity is markedly increased because many Xe cages are assembled into the same nanoparticle (the detection limit of the assembled capsid is 70 pM).

1.2. Recent advances in dissolution DNP

DNP is a hyperpolarization method [13,14] that can be used, in principle, to hyperpolarize any molecule, but, to achieve high efficiency, special conditions have to be met. First of all, a homogeneous solid solution of the radical and the substrate to be polarized has to be obtained; i.e., crystallization of the sample must be avoided and formation of a glassy solid is necessary. Ardenkjær-Larsen has reported the use of new paramagnetic radicals and the dependence of polarization on magnetic field strength (3.35 and 4.64 T) [15,16]. He also showed that the addition of a

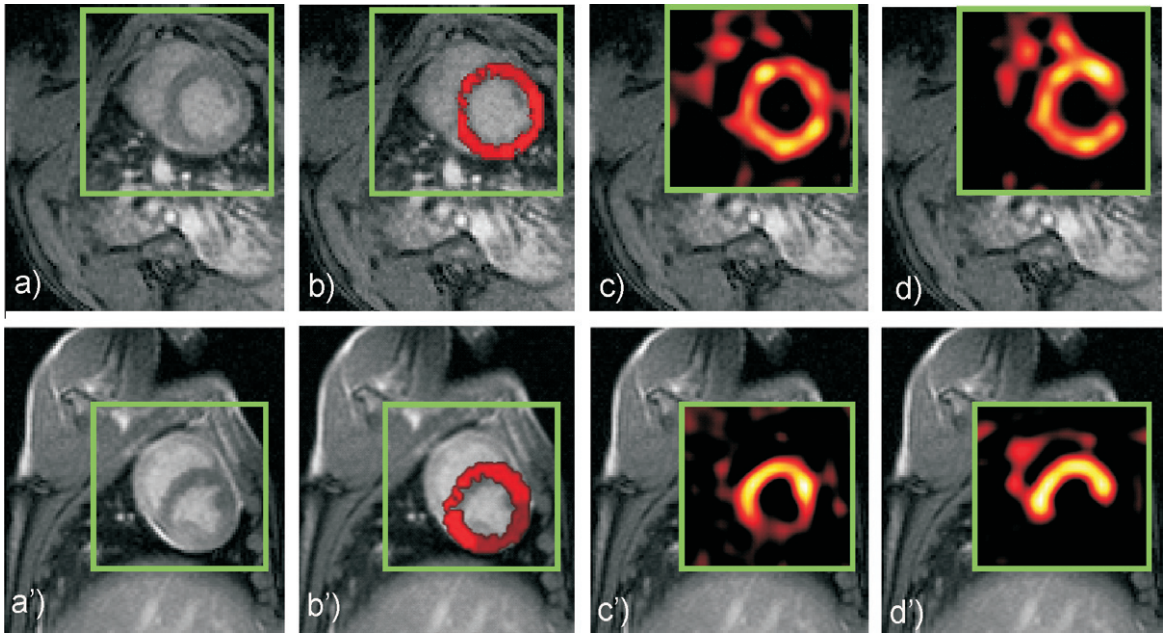

Fig. 1. Cardiac metabolic imaging of a pig heart after occlusion with a balloon: (a) proton image, (b) Gd perfusion, (c) ^{13}C image of alanine, (d) bicarbonate image. The four upper images have been acquired after 15′ occlusion, the lower after 45′ occlusion. While nothing is observed in the proton images, diminished carbonate production is evident in the ^{13}C CSI hyperpolarized images.

small amount of Gd^{3+} in the solid glassy solution enables high polarization transfer to organic molecules.

Among the several biologically relevant molecules that have been hyperpolarized using DNP, the most promising and significant results deal with the use of pyruvate. This molecule lies at the crossing of different metabolic pathways and can be used as an indicator of different enzymatic activities and, in turn, of the viability of cells [17–19].

Very interestingly, at WWMR2010, the use of ^{13}C hyperpolarized pyruvate as an indicator of heart activity under normal and abnormal metabolic conditions (ischemic episodes, diabetes) was also reported [20]. Hyperpolarized ^{13}C chemical shift imaging makes it possible to monitor the pyruvate flux through the enzyme pyruvate dehydrogenase (PDH), which, in its activated form, quickly converts pyruvate into CO_2, which is in rapid equilibrium with carbonate. Altered plasma compositions, induced in the presence of a diseased state, can alter the activity of PDH, which can then be investigated through the production of hyperpolarized HCO_3^-/CO_2 [21]. Changes in the cardiac metabolic pathway induced by ischemic episodes have been monitored by acquiring CSI images of the signals of bicarbonate, lactate, and alanine before and after occlusion of the left circumflex artery of pigs (Fig. 1). It was observed that after 15 min of occlusion the only change is a diminished carbonate signal, while after 45 min the carbonate production is almost zeroed and alanine is also diminished. The production of alanine in the cardiac tissue demonstrates that, in spite of the occlusion, the tissue is still alive, while the reduced carbonate signal corresponds to lowered activity of the Krebs cycle. Furthermore, the activity recovers 2 h after the removal of the occlusion, thus yielding relevant information about the long-term effect on the mitochondria. Metabolic images using hyperpolarized pyruvate may then provide information about cellular damage, perfusion, and the citric acid cycle superior to the diagnostic content of currently available nuclear-medicine-based tests.

DNP with HP pyruvate appears to be a real breakthrough in medical diagnosis. Nelson's lecture was expected to reveal that the outstanding preclinical achievements have been successfully translated to human beings. Unfortunately, this was not the case, because regulatory issues have delayed the start of clinical trials at the University of California, San Francisco. However, a few months later at RSNA 2010 (the Radiological Society of North America), the first human results were reported to confirm the great expectations for this innovative diagnostic method from the preclinical work.

Another substrate that is currently under intense scrutiny [22] is hyperpolarized 1,4-^{13}C fumarate. It has been shown that the detection of its metabolism provides a tool for assessing cellular necrosis as a tumor response to treatment. In fact, its hydration to malate is more evident in treated tumor cells than in untreated ones.

Another particularly important achievement that was discussed at the conference was the use of hyperpolarized bicarbonate ($H^{13}CO_3^-$) [23] for in vivo pH assessment from $H^{13}CO_3^-/CO_2$ polarized signals ratio (Fig. 2). Because many pathologies are characterized by variations of tissue pH, the administration of polarized bicarbonate would provide a powerful and harmless tool for detecting disease and response to treatment.

1.3. Parahydrogen-induced polarization

While DNP and optical pumping of noble gases strongly rely on the availability of complex technologies, parahydrogen-induced polarization makes it possible to obtain hyperpolarized products by means of a simple chemical reaction between parahydrogen and organic molecules.

At WWMR2010, Duckett and co-workers [24] reported a new approach using parahydrogen developed at the University of York. The method has been named SABRE (signal amplification by reversible exchange) and represents outstanding progress in hyperpolarization. This method does not imply the addition of parahydrogen to the substrate, but polarization transfer is achieved thanks to the formation of a ternary adduct between an organometallic Ir(I) complex, the coordinated parahydrogen moiety, and an organic substrate that is capable of reversible coordination at the metal center. The Ir(I) complex $([Ir(COD)PCy_3Py]^+[BF_4]^-$ and other analogous complexes with different coordinating phosphines) reacts with molecular hydrogen to form a dihydride complex ($[H_2IrPR_3Py]^+$) in equilibrium with a nonhydrogenated one. The dihydride complex is able to reversibly coordinate pyridine or other ligand molecules (e.g., nicotine, quinoline). Upon formation of the adduct, a unique spin system that involves the two polarized hydrides from the parahydrogen molecule and all the nuclei of the ligand is obtained and polarization can flow through the scalar coupling network. Signal enhancement has been detected not only on protons but also on ^{13}C and ^{15}N of the substrate molecules. The intensity of polarization transferred to the ligand depends on the exchange rate of parahydrogen and of the ligand itself. Signal enhancement is also a (nonlinear) function of the intensity of the magnetic field in which the hyperpolarization process is carried out. In particular, it was observed that the amount of transferred polarization changes markedly when the field increases from 0.5×10^{-3} (earth magnetic field) to 1×10^{-2} T (spectrometer fringe field). Interestingly, no magnetization transfer occurs when the magnetic field strength is higher than 1 T. The signal enhancement till now obtained with SABRE can go up to 500 for protons and 800 for carbon. The method offers an outstanding perspective on parahydrogen polarization, which is now no longer limited to the use of unsaturated, easily hydrogenatable molecules, but can be applied to other classes of compounds that enter the coordina-

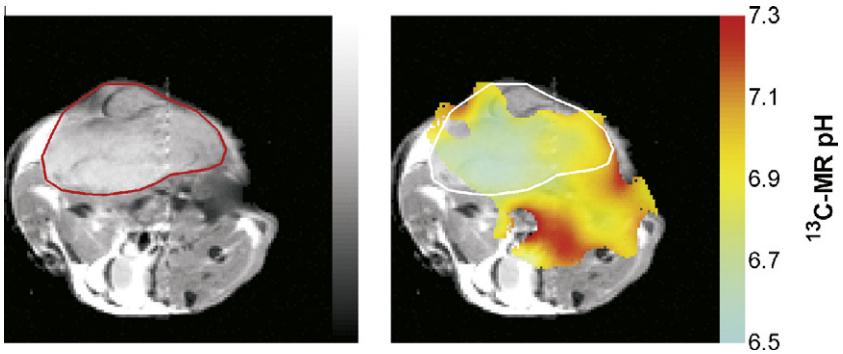

Fig. 2. Image of a tumor pH in vivo: (a) proton image of a tumor (outlined in red) implanted in a mouse; (b) pH map calculated from the ratio of $H^{13}CO_3^-$ and CO_2.

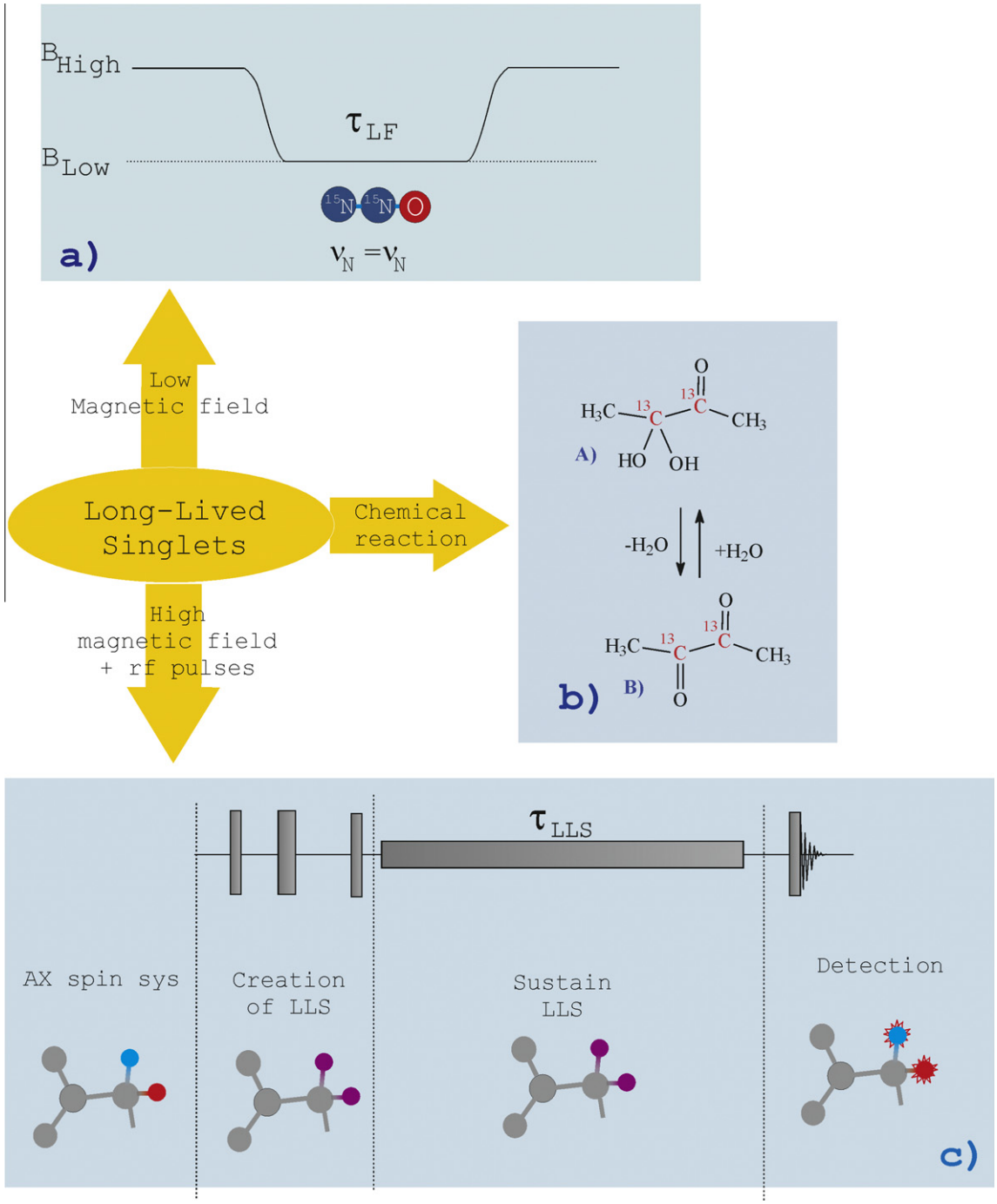

Fig. 3. The possibility of store hyperpolarization in long-lived singlet states has been investigated using different methods: (a) changing the magnetic field strength: in fact, in a two-spin system such as $^{15}N_2O$, the singlet state can be reversibly formed and destroyed by moving the sample from high field to earth field and back (Levitt); (b) by a chemical reaction: the two ^{13}C nuclei of $^{13}C_2$ diacteyl (A) are nonequivalent, while in the dehydrated form (B) they are equivalent and a singlet state is formed (Warren); (c) at high field, in the spectrometer, the long-lived state, i.e., zero quantum coherence, is excited by an appropriate pulse sequence, and then is maintained by RF irradiation during τ_{LLS} (Levitt and Bodenhausen).

tion sphere of the metal center at which para-H_2 is reversibly coordinated.

1.4. Polarization lifetime: how can this problem be addressed?

Whatever the polarization technique used, signal enhancement from the hyperpolarized species has a transitory nature and its duration depends on the relaxation rate of the polarized nucleus. Therefore a great deal of effort has been focused on the search for methods for extending the lifetime of the polarized species (Fig. 3).

A key idea for extending polarization duration beyond the T_1 limit has been introduced by Levitt and co-workers [25]. It relies on the fact that dipole–dipole relaxation processes do not affect singlet states, which are isolated from the other spin states. Two methods for obtaining a singlet state on molecules containing a pair of nonequivalent spins have been proposed. The first is based on the fact that a singlet state $S = |\alpha\beta - \beta\alpha\rangle$ can be reversibly formed and destroyed simply by moving the sample from high to

low field and back. The effect of these long-lived singlet states (LLS) is really stunning in the case of $^{15}N_2O$, where the nonequilibrium state induced in the two chemically different ^{15}N nuclei was maintained for 300 s at low magnetic field.

The second achieves a singlet state at high magnetic field by designing a proper pulse sequence. An experiment was set up by Caravetta and Levitt [26] in which a molecule containing two different protons was irradiated, after the excitation of ZQ coherence, with an unmodulated frequency (CW irradiation). It was shown that the T_1 of the singlet state maintained by the RF irradiation is much longer (more than 10 times) than the decay time constant of the two protons.

Another way to a obtain a singlet state that can be reversibly switched into a magnetically active state is a chemical method discussed at WWMR2010 by Warren et al. [27]. It relies on the fact that two magnetically active nuclei can be chemically equivalent or not in two different forms of the same molecule. In the example worked out by Warren and co-workers, the hydrated and the dehydrated forms of 2,3-^{13}C diacetyl were considered. In the hydrated form the two ^{13}C differ by 110 ppm, while in the dehydrated form they are equivalent, thus forming a singlet state that is disconnected from the other spin states. Therefore a nonequilibrium, polarized spin state can be created in the hydrated form and the dehydrated form can be obtained by changing the solvent polarity, i.e., by adding acetone to the solution. In the latter form the two ^{13}C nuclei form a true singlet state that, being completely isolated from the other states, is a long-lived state. An increased signal is observed upon to unlocking of the diacetyl singlet state when water is added to the acetone solution.

The high ^{13}C signal enhancement attained in a DNP experiment can benefit from the long-lived singlet state effect, thanks to a new approach introduced by Bodenhausen and co-workers [28,29] to convert hyperpolarized ^{13}C magnetization into a LLS. This was achieved on the natural abundance ^{13}C signal of the dipeptide Gly–Ala, enhanced by four orders of magnitude by means of DNP. Then, by a tailored pulse sequence, polarization is transferred to the nonequivalent pair of protons (^{a}H) J coupled to the glycine ^{13}C and here stored as a long-lived singlet. Finally, after storage, part of the polarization can be extracted and observed. The relaxation rate of LLS was found to be about seven times slower than the corresponding T_1 kinetics of the two protons. Furthermore, the detection of the ^1H signal is more sensitive than for ^{13}C. The proposed method opens new horizons in the exploitation of hyperpolarized molecules for the investigation of slow metabolic processes.

2. Advances in MRI acquisition methods

Ultra-fast MRI approaches make it possible to obtain a whole image in a single scan and have wide application in functional MRI and diffusion studies. The main drawback of these methods, the most common of which is echo-planar imaging (EPI), is that they suffer from distortion effects due to susceptibility variations in the sample and to chemical shift distributions. These drawbacks are linked to the relatively long data-sampling time that characterizes the EPI sequence. In fact, in this kind of experiment, a single pulse is used to excite all the spins; then a large phase-encoding gradient is rapidly switched to form echoes that to build the image. Therefore, highly inhomogeneous regions with very low T_2^* cannot be well characterized, and various chemical sites can generate highly distorted signals due to chemical shift artifacts.

Frydman and co-workers at Weizmann are developing a new MRI technique, which is based on spatial encoding of the spins instead of frequency encoding [30,31]. This same principle has already been applied to MR spectroscopy to obtain multidimensional MR spectra in a single scan. The spatial encoding of spins is achieved by applying a magnetic field gradient (G_{exc}) that spreads out the frequencies in the sample and a frequency-incremented pulse instead of a hard pulse as in classical FT imaging and spectroscopy. By sweeping the focus of the pulse, spatially progressive spin excitation is achieved, and the spin density profile along the same axis of the gradient ($\rho(y)$) is reconstructed directly from the magnitude of the $S(t)$ signal acquired in the presence of a G_{acq} gradient such that $|G_{exc}T_{exc}| = |G_{acq}T_{acq}|$. The spatial encoding thus obtained does not require FT to deliver the spatial information and makes it possible to avoid artifacts due to field inhomogeneities. The method also makes it possible to differentiate between chemical shift contributions to an image, as in the case of tissues containing both fat and water, with distortion effects in the EPI images when placed at high magnetic field. Using the proposed spatial encoding method, it is possible to filter chemical shift from the image and to obtain separate images from each of the resolved chemical specimens.

The spatially encoded images suffer from poor spatial resolution because the pixel size is determined by the relatively short excitation process and not by the acquisition time, as in all the other imaging methods. To face this problem, superresolution (SR) algorithms have been used, which make possible improved image resolution on the basis of oversampling considerations. In fact, the space-encoding method provides redundancy in information because the displacement of the focus of the spins having their magnetization in phase at a certain time point ($S(t)$) (which form the signal) is small and there is overlap between successive acquisition events. The redundancy of information is exploited to improve the spatial resolution of the image.

Fast MRI acquisition is very important for visualizing a number of physiological processes such as heartbeats or joint movements and for monitoring therapeutic interventions in real time. Many frames must be sampled per second to avoid discontinuities, and spatial resolution will not be high. EPI has limited spatial resolution, imposed by the duration of the echo train. Furthermore, the long data acquisition time that characterizes EPI makes it very sensitive to magnetic field inhomogeneities, which can be present in many regions of the body due to surgical instruments or air-filled cavities. The solution presented by Fraham et al. [32] combines a fast low-angle shot (FLASH) technique with a radial sampling of the data in k-space and an image reconstruction method that can reduce the temporal resolution below the acquisition time of one full image. Classical sampling of the data proceeds in a linear (Cartesian) way; i.e., rows of the k-space are covered progressively, and the image is formed only when the central part of the k-space, containing the low spatial frequencies, is formed. Then the image can be updated after a relatively long time delay, which is not compatible with monitoring fast physiological processes, as in cardiac MRI. On the contrary, radial acquisition of the data, which is achieved using a phase-encoding gradient obtained by combining G_x and G_y gradients, makes it possible to obtain spokes (in the k-space) that contain both high and low spatial frequencies; therefore temporal discontinuities are considerably reduced. The acquisition of the whole data set requires the acquisition of several spokes, in order to cover 360°; however, a reduction in the number of spokes does not influence the spatial resolution of the image, but the signal-to-noise ratio. To further decrease the time delay between successive frames, sharing of partial datasets from successive images was applied. In practice, the total number of spokes used to acquire an image was divided into groups of interleaves, each covering the whole space with a fraction of the total spokes, and each interleaf can be shared between successive images [33]. This trick makes it possible to shorten the image update with respect to the time of acquisition of the whole image. For instance, the acquisition of a cardiac image with in-plane resolution 2×2 mm, can be acquired using 125 spokes for each image, which

takes 250 ms. If the spokes are arranged in five groups of 25 spokes (five interleaves), each covering the whole data space, it is possible to update the image every 50 ms. In fact, it has been possible to perform cardiac MRI with high spatial resolution at a rate of 20 frames per second. Radial FLASH MRI appears to be the most suitable method for the investigation of cardiac functions, joint movements, interventional MRI, and dynamic contrast agent perfusion.

The acquisition of images of spins with very short transverse relaxation time (<1 ms), such as semisolids or surrounding superparamagnetic particles, using tradition FT imaging methods is particularly challenging. The echo time can further exceed the T_2^* of these spins, and the signal from these regions is completely lost before the acquisition is started. Furthermore, the presence of strongly paramagnetic particles generates large dipolar fields in the neighboring regions that are then obscured. In other words, T_2^* shortening, which can have different origins, produces dark spots with low signal-to-noise ratio and poor specificity. The method called SWIFT (sweep imaging with Fourier transform) developed by Garwood and co-workers [34,35] makes it possible to circumvent the drawbacks of the echo time in traditional FT imaging by introducing almost simultaneous excitation and acquisition of the spins. This is made possible by the fact that the excitation pulses are frequency modulated (in fact, frequency-swept excitation pulses are used) and each pulse is divided into N units. A single unit is formed by a RF pulse of duration τ_p, after which, when the RF power is off, the signal is acquired. Therefore pulse and acquisition are practically simultaneous. During a pulse, both excitation and acquisition are carried out in the presence of a magnetic field gradient ($G_x + G_y + G_z$) that makes it possible to spatially encode the spins. The gradients are gradually stepped between successive pulses in order to acquire a full set of frequency-encoding projections. The SWIFT method has been shown to allow the acquisition of images from water molecules around strongly paramagnetic materials (Ti balls in water) and from stem cells labeled with SPIO particles [36]. SWIFT images make possible retention of the signal derived from regions with very short T_2^* that give positive contrast, as the quick sampling of the data after each pulse element makes it possible to observe the signals of fast relaxing spins. The high contrast provided by this method has been exploited for the detection of stem cells labeled with paramagnetic particles.

3. Advances in molecular imaging

Molecular imaging is broadly defined as the (quantitative) visualization of molecules and of molecular events that occur at cellular level. Compared with other imaging modalities, MRI suffers from the limited sensitivity of its probes. Therefore, while awaiting fallout from hyperpolarization methods, much current work is still devoted to designing strategies to enhance the response of MRI probes in molecular imaging studies. As far as concerns the paramagnetic systems, much attention is still devoted to the design of Gd-based contrast agents to optimize the determinants of the relaxivity. Botta [37] and Meade [38] reported the rational design of new Gd systems that, through optimized control of the hydration sphere around the paramagnetic metal center and overall control of the molecular reorientation rate, show relaxivities markedly higher than those currently available with commercial agents.

It was established early that the binding of a paramagnetic complex to a slowly moving target yields a relaxivity peak centered at ca. 35–40 MHz. For this reason, paramagnetic agents display maximum efficiency on MRI scanners operating in the range 0.5–1.5 T rather than at higher fields. At WWMR2010, Rutt et al. [39] discussed a smart exploitation of this property of paramagnetic macromolecular systems. The method is named dreMR (delta-relaxation-enhanced MR), and it aims at sensitizing images to the slope of relaxation vs B_0 by field cycling around a given value of the static field. The dreMR experiment can be performed on existing MRI scanners with some additional field cycling hardware. Thus, by acquiring two images at ±60 mT on a 1.5-T scanner, one can take advantage of being on the slope of the relaxivity peak generated by a Gd agent bound to a protein.

As far as concerns the probe design, interesting developments have been reported also for the new class of CEST agents. Differently from paramagnetic systems, CEST agents yield (negative) contrast enhancement through the transfer of saturated magnetization from a pool of exchangeable protons of the contrast agent to the "bulk" water signal. To improve the sensitivity of these agents, Delli Castelli and co-workers [40,41] proposed to use, as an exchangeable pool of protons, the ensemble of water molecules that are entrapped in the aqueous cavities of liposomes. To make the intravesicle water signal different from the bulk water resonance, they suggested the co-entrapment of a lanthanide shift reagent. Furthermore, the shift of the intraliposome water signal increased further when the shape of the liposome particle changed from spherical to ellipsoidal. Control of the determinants of the shift of the water signal has allowed the generation of several CEST agents, each characterized by a specific absorption frequency of the entrapped water. CEST agents represent important progress in the field, as, being frequency-encoding systems, they can be interrogated "at will," providing multiplex (e.g. multicolor) applications that were not possible with classical relaxation agents.

Many molecular imaging applications were presented at the conference. Neeman [42] investigated in depth the microenvironmental control of vascular remodeling in angiogenesis by designing a number of functional, molecular, and cellular methods to characterize newly formed vasculature in the early stage of fetal implantation and during the early stage of tumor growth.

Nicolay [43] has shown how the use of targeted nanoparticles may make it possible to overcome sensitivity issues for the in vivo MR detection of sparse molecular markers. He surveyed the major routes to equipping the nanoparticle with a high payload of MRI contrast agent, namely, (i) nanoparticles loaded with Gd^{3+} chelates for T_1 shortening; (ii) FeO nano-crystals for T_2 detection, (iii) fluorinated nano-emulsions for F-19MRI, and (iv) nanoparticles incorporating CEST agents.

Whereas many efforts have been devoted to designing highly sensitive probes for visualizing molecular targets, it is worth noting the achievements in understanding the endogenous contrast in terms of the chemical forms that determine it. In this context, Mitsumori et al. [44,45] have shown that the apparent relaxation rate of tissue water in the human brain is well explained in terms of a linear combination of [Fe] and f_M(=1 − water fraction):

$$R_2 = \alpha[\mathrm{Fe}] + \beta f_M + \gamma,$$

where α is linearly dependent on B_0 and is determined by the same mechanisms operating for ferritin solutions; β is quadratically dependent on B_0 and represents the contribution arising from the dynamic dephasing mechanism; and γ is mostly independent of B_0 and represents the classical dipolar relaxation contribution.

Along the line of reasoning on how much information can currently be attained in bio-imaging investigations, we recall the work of Rudin and co-workers [46,47] as a representative example of the state of the art. They have applied f-MRI to analyze the functional reorganization following focal CNS lesions in rats and highlighted the potential of f-MRI in studying genetically engineered mice. As the principal challenge in mouse f-MRI is sensitivity, they showed that the use of low-temperature MRI detection coils yields highly reproducible f-MRI responses to sensory inputs on anesthetized mice.

4. Concluding remarks

Although in a very concise manner, we hope that the contributions reported in this survey offer a taste of the advances in biomedical spectroscopy and imaging shown at WWMR2010. The work presented at the Conference shows that NMR spectroscopy and imaging in vivo are far from being a mature science, and innovative solutions in methods and applications are continuing to be developed. These efforts will further strengthen the key role of NMR in biology and medicine.

References

[1] R.R. Rizi, Assessment of Lung Function with Polarized MRI, WWMR2010 Book of Abstracts, p. 86.
[2] E.E. deLange, J.P. Mugler, J.R. Brookeman, J. Knight-Scott, J.D. Truwit, C.D. Teates, T.M. Daniel, P.L. Bogorad, G.D. Cates, Lung air space: MR imaging evaluation with hyperpolarized ^{3}He gas, Radiology 856 (1999) 851–857.
[3] I.E. Dimitrov, E. Insko, R. Rizi, J.S. Leigh, Indirect detection of lung perfusion using susceptibility-based hyperpolarized gas imaging, Magn. Reson. Imag. 21 (2005) 149–155.
[4] J. Yu, M. Law, S. Kadlecek, K. Emami, M. Ishii, M. Stephen, J.M. Woodburn, V. Vahdat, R. Rizi, Simultaneous measurement of pulmonary partial pressure of oxygen and apparent diffusion coefficient by hyperpolarized ^{3}He MRI, Magn. Reson. Med. 61 (2009) 1015–1021.
[5] B. Driehuys, Recent Progress in Clinical Hyperpolarized ^{129}Xe MRI, WWMR2010 Book of Abstracts, p. 40.
[6] B. Driehuys, J. Pollaro, G.P. Cofer, In vivo MRI using real-time production of hyperpolarized ^{129}Xe, Magn. Reson. Med. 60 (2008) 14–20.
[7] R.T. Branca, Z.I. Cleveland, B. Fubara, C.S.S.R. Kumar, R.R. Maronpot, C. Leuschner, W.S. Warren, B. Driehuys, Molecular MRI for sensitive and specific detection of lung metastases, PNAS 107 (2010) 3693–3697.
[8] M.M. Spence, S.M. Rubin, I.E. Dimitrov, E.J. Ruiz, D.E. Wemmer, A. Pines, S.Q. Yao, F. Tian, P.G. Schultz, Functionalized xenon as a biosensor, PNAS 98 (2001) 10654–10657.
[9] L. Schroder, T. Lowery, C. Hilty, D.E. Wemmer, A. Pines, Molecular imaging using a targeted magnetic resonance hyperpolarized biosensor, Science 314 (2006) 446–449.
[10] L. Schroder, T. Meldrum, F. Schilling, D.E. Wemmer, A. Pines, Encapsulated Xenon as an NMR Sensor for Biochemical Applications, WWMR2010 Book of Abstracts, p. 89.
[11] L. Schroder, L. Chavez, T. Meldrum, M. Smith, T.J. Lowery, D.E. Wemmer, A. Pines, Temperature-controlled molecular depolarization gates in nuclear magnetic resonance, Angew. Chem. Int. Ed. 47 (2008) 4316–4320.
[12] T. Meldrum, K.L. Seim, V.S. Bajaj, K.K. Palaniappan, W. Wu, M.B. Francis, D.E. Wemmer, A. Pines, A Xenon-based molecular sensor assembled on an MS2 viral capsid scaffold, J. Am. Chem. Soc. 132 (2010) 5936–5937.
[13] K. Golman, Polarization: Possibilities and Impossibilities, WWMR2010 Book of Abstracts, p. 50.
[14] J.H. Ardenkjær-Larsen, B. Fridlund, A. Gram, G. Hansson, L. Hansson, M.H. Lerche, R. Servin, M. Thaning, K. Golman, Increase in signal-to-noise ratio of >10000 times in liquid state NMR, PNAS 100 (2003) 10158–10163.
[15] J.H. Ardenkjaer-Larsen, New Developments in Dissolution-DNP for in Vivo Imaging, WWMR2010 Book of Abstracts, p. 18.
[16] S. Macholl, H. Johannesson, J.H. Ardenkjaer-Larsen, Trityl biradicals and ^{13}C dynamic nuclear polarization, Phys. Chem. Chem. Phys. 12 (2010) 5804–5817.
[17] K. Golman, R. Zandt, M. Thaning, Real time metabolic imaging, PNAS 103 (2006) 11207–11275.
[18] S.J. Nelson, In Vivo Applications of MR Physiological and Metabolic Imaging, WWMR2010 Book of Abstracts, p. 13.
[19] M.J. Albers, R. Bok, A.P. Chen, C.H. Cunningham, M.L. Zierhut, V.Y. Zhang, S.J. Kohler, J. Tropp, R.E. Hurd, Y. Yen, S.J. Nelson, D.B. Vigneron, J. Kurhanewicz, Hyperpolarized ^{13}C lactate, pyruvate and alanine: noninvasive biomarkers for prostate cancer detection and grading, Cancer Res. 68 (2008) 8607–8615.
[20] K. Golman, J.S. Petersson, P. Magnusson, E. Johansson, P. Akeson, C.M. Chai, G. Hansson, S. Mansson, Cardiac metabolism measured noninvasively by hyperpolarized ^{13}C MRI, Magn. Reson. Med. 59 (2008) 1005–1013.
[21] M.A. Schroder, L.E. Cochlin, L.C. Heather, K. Clarke, G.K. Radda, D.J. Tyler, In vivo assessment of pyruvate dehydrogenase flux in the hearth using hyperpolarized carbon-13 magnetic resonance, PNAS 105 (2008) 12051–12056.
[22] F.A. Gallagher, M.I. Kettunen, D. Hu, P.R. Jensen, R. Zandt, M. Karlsson, A. Gisselsson, S.K. Nelson, T.H. Witney, S.E. Bohndiek, G. Hansson, T. Peitersen, M.H. Lerche, K.M. Brindle, Production of hyperpolarized [1,4-$^{13}C_2$]malate from [1,4-$^{13}C_2$]fumarate is a marker of cell necrosis and treatment response in tumors, PNAS 106 (2009) 19801–19806.
[23] F. Gallagher, M.I. Kettunen, S.E. Day, J.H. Ardenkiaer-Larsen, R. Zandt, P.R. Jensen, M. Karlsson, K. Golman, M.H. Lerche, K. Brindle, Magnetic resonance imaging of pH in vivo using hyperpolarized ^{13}C-labelled bicarbonate, Nature 453 (2008) 940–943.
[24] R.W. Adams, K.D. Atkinson, M.J. Cowley, S.B. Duckett, G.R. Green, R.A. Green, R. Mewis, D. Williamson, Transfer of Parahydrogen Derived Spin Order Sensitizes MRI and NMR Measurements by Three Orders of Magnitude, WWMR 2010 Book of Abstracts, p. 41.
[25] M. Carravetta, O.G. Johannessen, M.H. Levitt, Beyond the T_1 limit: singlet nuclear spin states in low magnetic fields, Phy. Rev Lett. 92 (2004) 153003-1–153003-4.
[26] M. Carravetta, M.H. Levitt, Long lived nuclear spin states in high field solution NMR, J. Am. Chem. Soc. 126 (2004) 6228–6229.
[27] W. Warren, E. Jenista, R.T. Branca, X. Chen, Increasing polarization spin lifetimes through true singlet states, Science 323 (2009) 1711–1714.
[28] R. Sarkar, P. Ahuja, P.R. Vasos, G. Bodenhausen, In Search of Line Narrowing, Extended Spin Memory and Enhanced Polarization: Through the Looking Glass of NMR, WWMR2010 Book of Abstracts, p. 101.
[29] P.R. Vasos, A. Comment, R. Sarkar, P. Ahuja, S. Jannin, J.-P. Ansermet, J.A. Konter, P. Hautle, B. van den Brandt, G. Bodenhausen, Long-lived states to sustain hyperpolarized magnetization, PNAS 106 (2009) 18469–18473.
[30] N. Ben-Eliezer, L. Frydman, Payback Time: Spatially Encoded NMR as a Novel MR Imaging Modality-Principle and Prospects, WWMR2010 Book of Abstracts, p. 45.
[31] A. Tal, L. Frydman, Spectroscopic imaging from spatially-encoded single-scan multidimensional MRI data, J. Magn. Reson. 189 (2007) 46–58.
[32] J. Fraham, M. Uecker, S. Zhang, Magnetic Resonance Imaging in Real Time, WWMR2010 Book of Abstracts, p. 44.
[33] S. Zhang, K.T. Block, J. Fraham, Magnetic resonance imaging in real time: advances using radial FLASH, J. Magn. Reson. Imag. 31 (2010) 101–109.
[34] M. Garwood, D. Idiyatullin, C. Corum, S. Moeller, R. Chamberlain, R. O'Connell, D. Sachdev, D. Nixdorf, Frequency-swept MRI: No Sound or Echoes, WWMR2010 Book of Abstracts, p. 47.
[35] D. Idiyatullin, C. Corum, S. Moeller, M. Garwood, Gapped pulses for frequency-swept MRI, J. Magn. Reson. 193 (2008) 267–273.
[36] R. Zhou, D. Idiyatullin, S. Moeller, C. Corum, H. Zhang, H. Qiao, J. Zhong, M. Garwood, SWIFT detection of SPIO-labelled stem cells grafted in the myocardium, Magn. Reson. Med. 63 (2010) 1154–1161.
[37] M. Botta, Optimizing the Relaxivity of Macromolecular MRI Contrast Agents, WWMR2010 Book of Abstracts, p. 25.
[38] T.J. Meade, The Coordination Chemistry of Signal Amplification and Targeting for MR probe Development, WWMR2010 Book of Abstracts, p. 74.
[39] B. Rutt, J. Rao, G. Liang, N. Ma, M.L. Ma, D. Ye, J. Roland, Y. Chen, Controlled Self Assembly of Nanoparticles: A General Template for Developing "Smart" MRI Contrast Agents, WWMR2010 Book of Abstracts, p. 87.
[40] D. Delli Castelli, E. Terreno, W. Dastrù, S. Aime, Magnetically Oriented Nanovesicles as MRI CEST Agents, WWMR2010 Book of Abstracts, p. 281.
[41] E. Terreno, C. Cabella, C. Carrera, D. Delli Castelli, R. Mazzon, S. Rollet, J. Stancanello, M. Visigalli, S. Aime, From spherical to osmotic shrunken paramagnetic liposomes: an improved generation of LIPOCEST MRI agents with highly shifted water protons, Angew. Chem. Int. Ed. 46 (2007) 966–968.
[42] M. Neeman, Imaging Angiogenesis: Microenvironmental Control of Vascular Remodeling, WWMR2010 Book of Abstracts, p. 77.
[43] K. Nicolay, The Challenges and Opportunities of Molecular Imaging with MRI, WWMR2010, Book of Abstracts, p. 77.
[44] F. Mitsumori, H. Watanabe, N. Takana, M. Garwood, E.J. Auerbach, Towards Understanding Transverse Relaxation Mechanisms of Tissue Water in Human Brain, WWMR2010 Book of Abstracts, p. 291.
[45] F. Mistumori, H. Watanabe, N. Takana, Estimation of brain iron concentration in vivo using a linear relationship between regional iron and apparent transverse relaxation rate of the tissue water at 4.7T, Magn. Reson. Med. 62 (2009) 1326–1330.
[46] S. Sosshard, A. Schroeter, E. Sydekum, M. Rudin, Adaptive Changes in Brain Function in Response to Pathological and Physiological Challenges: f-MRI in Rodents to Assess Plasticity in CNS, WWMR2010 Book of Abstracts, p. 86.
[47] A. Gosh, F. HAiss, E. Sydekum, R. Schneider, M. Gullo, M.T. Wyss, T. Mueggler, C. Baltes, M. Rudin, B. Weber, M.E. Schwab, Rewiring of hindlimb corticospinal neurons after spinal cord injury, Nat. Neurosci. 23 (2009) 97–104.